X. Liu
R. E. DeVor
S. G. Kapoor

Department of Mechanical and Industrial Engineering
University of Illinois at Urbana-Champaign,
Urbana, IL

K. F. Ehmann
Department of Mechanical Engineering,
Northwestern University,
Evanston, IL

The Mechanics of Machining at the Microscale: Assessment of the Current State of the Science

This paper provides a comprehensive review of the literature, mostly of the last 10–15 years, that is enhancing our understanding of the mechanics of the rapidly growing field of micromachining. The paper focuses on the mechanics of the process, discussing both experimental and modeling studies, and includes some work that, while not directly focused on micromachining, provides important insights to the field. Experimental work includes the size effect and minimum chip thickness effect, elastic-plastic deformation, and microstructure effects in micromachining. Modeling studies include molecular dynamics methods, finite element methods, mechanistic modeling work, and the emerging field of multiscale modeling. Some comments on future needs and directions are also offered. [DOI: 10.1115/1.1813469]

1 Introduction

Emerging miniaturization technologies are potentially key technologies of the future that will bring about completely different ways people and machines interact with the physical world. The miniaturization of devices is today demanding the production of mechanical components with manufactured features in the range of a few to a few hundred microns in fields that include optics, electronics, medicine, biotechnology, communications, and avionics, to name a few. Specific applications include microscale fuel cells, fluidic microchemical reactors requiring microscale pumps, valves and mixing devices, microfluidic systems, microholes for fiber optics, micronozzles for high-temperature jets, micromolds, deep X-ray lithography masks, and many more [1–11]. Some examples of micromachined features and parts are shown in Fig. 1. These applications require very tight tolerances, and both functional and structural requirements demand the use of various engineering materials, including stainless steel, titanium, brass, aluminum, platinum, iridium, plastics, ceramics, and composites.

While an enormous amount of manufacturing process development, e.g., wet etching, plasma etching, LIGA, etc., has taken place in the last two to three decades as a result of the explosion of activities in microelectromechanical systems (MEMS), such development suffers from several limitations that encumber the use of these methods to address the aforementioned needs. In particular, MEMS-based methods are directed toward silicon and siliconlike materials and are basically planar $2\frac{1}{2}$-D processes. Furthermore, relative accuracies (tolerance-to-feature size) are of the order of 10^{-1} to 10^{-2}, whereas the needs of many emerging miniaturization applications require relative accuracies in the 10^{-3} to 10^{-5} range in a wide range of materials for parts that have true three-dimensional (3D) free-form surface features. Processes such as machining can, in principle, meet these needs, but there are a number of scientific and technological challenges that must be overcome if machining processes and equipment are to emerge that can respond in a technically sound, economic, and reliable fashion.

There are a number of issues that prevail in microscale machining that are fundamentally different from macroscale machining and influence the underlying mechanisms of the process, resulting in changes in the chip-formation process, cutting forces, vibrations and process stability, and the generation and subsequent character of the resulting machined surface. For example, the tool geometry, viz., edge radius, is comparable in size to the cutting geometry, viz., chipload, owing to the current status of economic microtool manufacturing methods. As a result, the effective rake angle becomes highly negative [12,13], which, in turn, causes ploughing and associated elastic-plastic deformation of the workpiece material to become much more dominant factors in the process. In fact, if the chipload is of the same order or less than the edge radius of the tool, then a chip may not be formed during each tooth passing. This phenomenon, known as the minimum chip thickness effect [14–17], has a profound impact on the cutting forces, process stability, and resulting surface finish in microscale machining. In processes such as endmilling, where the chipload varies during a single engagement of a tooth in the cut, the cutting mechanism may change from ploughing-dominated to shearing-dominated and back to ploughing-dominated again within a single excursion of a tooth through the cut. Furthermore, owing to the very small chiploads in micromachining, the well-known size effect plays a significant role.

In microscale machining the relationship of the cut geometry to the workpiece microstructure is also markedly different from macroscale machining. In microscale machining, where chiploads may range from submicron levels to a few microns and depths of cut may be in the range of a few microns to perhaps 100 μm, the cut geometry and the grain sizes of the workpiece material are now comparable in size. As a result when cutting ferrous materials, for example, the cutter engagement may be completely in ferrite, then pearlite, thereby significantly altering the cutting mechanisms and associated process response, e.g., forces and surface roughness. In [18], the authors noted significant frequency content in the experimental cutting force signal at wavelengths equal to the average grain size of the material being cut. Microstructural effects in microscale cutting are requiring quite different assumptions to be made concerning underlying material behavior during micromachining and have precipitated the need for new modeling approaches to account for such effects.

The objective of this paper is to provide a review of some of the more significant contributions to the literature that are now providing a fundamental understanding of the mechanisms that prevail in the world of microscale machining. While, in general, machining may include several processes, such as Electrical Discharge Machining (EDM), Electrochemical Machining (ECM), and laser machining, this paper focuses only on cutting processes. To this end, we will discuss both experimental and model-based studies, most of which have come to light in the last decade, and which together are laying the foundation for continuing research

Contributed by the Manufacturing Engineering Division for publication in the JOURNAL OF MANUFACTURING SCIENCE AND ENGINEERING. Manuscript received August 18, 2004; revised September 02, 2004. Associate Editor: S. N. Melkote

Fig. 1 (*a*) Micromilled trenches with stepped walls [8], (*b*) neurovascular device component, and (*c*) microgear

in this area. Some of the work reported here finds its origins in ultraprecision machining studies, but the majority of the work discussed is focused on the emerging field of microscale machining. This review begins with a discussion of experimental studies that have provided base-line data and a clearer picture of the mechanisms that dominate in micromachining. The paper then discusses a number of recent modeling and simulation efforts that both extend our understanding and provide more tractable ways to characterize and assess micromachining performance at this size scale. These include recent efforts using molecular dynamics simulation, microstructure-level finite element analysis, and mechanistic process modeling methods. Some aspects of the newly emerging field of multiscale modeling are also discussed.

2 Experimental Studies

In this section, a number of experimental studies are reviewed. Specific areas of focus include the size effect in micromachining and its impact on cutting forces, chip formation and morphology, and surface generation; the influence of built-up edge formation and elastic-plastic deformation while machining at this size-scale; and microstructure influences on machining performance at the microscale. Some of the relevant work cited finds its origins in the study of ultraprecision machining.

2.1 Size Effect

Cutting Force/Specific Cutting Energy. Lucca et al. [19] experimentally determined that the shearing process could not account for all of the observed energy when machining OFHC copper at small values of depth of cut. They showed that the ploughing and elastic recovery of the workpiece along the flank face of the tool play a significant role when machining with chip thickness values approaching the edge radii of the cutting inserts. They noticed that the specific cutting energy required to machine at very low chip-thickness values could not be explained by the energy required for shearing and for overcoming friction on the rake face of the tool. The significance of ploughing under these conditions was used to explain the increase in the cutting energy.

Later, Lucca and Seo [20] performed another experimental study of the effect of single-crystal diamond tool edge geometry (rake angle, tool edge radius) on the resulting cutting and thrust forces and specific energy in ultraprecision orthogonal flycutting on TECU®. Both the nominal rake angle and the tool edge profile were found to have significant effects on the resulting forces and energy dissipated over a range of uncut chip thicknesses from 20 μm to 10 nm. When the uncut chip thickness approaches the size of the edge radius, the effective rake angle appears to determine the resulting forces. This is predominantly shown by the study of the direction of the resultant force vector with respect to the uncut chip thickness as shown in Fig. 2. At small uncut chip thicknesses, the effective rather than the nominal rake angle dictates the direction of the resultant force.

Lucca et al. [21] performed diamond turning tests with ductile Al 6061-T6. They investigated the transition from a shearing-dominated cutting process to a ploughing-dominated process by studying the angle of the resultant cutting forces in orthogonal cutting. By using a diamond tool with a measured edge radius of approximately 200 nm, they found that at uncut chip thickness values less than the edge radius, the force per unit width in the thrust direction increases more rapidly than the force per unit width in the cutting direction. As the chip thickness decreases, the measured resultant force vector was found to be closer to the thrust direction than the cutting direction. The tool edge condition (tool wear) was found to have a significant effect on the thrust forces when the depth of cut was below the tool edge radius as shown in Fig. 3.

Taminiau and Dautzenberg [22] also witnessed an increase in cutting energy while machining brass with decreased chip thickness. Both rough cutting, using conventional tools with edge radii varying between 50 and 200 μm, and high-precision cutting, using a ground diamond tool with an edge radius of 15 μm, were carried out. The authors discovered that the specific cutting forces depended only on the ratio of the uncut chip thickness to the cutting edge radius when the uncut chip thickness was smaller than the edge radius. Based on the measured specific cutting energy, the yield shear stress of the workpiece material was estimated. The value of the yield shear stress in high-precision cutting was found to be almost twice as high as the value in conventional rough cutting for the same workpiece material. The authors attributed the difference to the presence of a higher strain rate in high-precision cutting.

Minimum Chip Thickness. Ikawa et al. [23,24] discussed the significance of the minimum thickness of a cut, which is defined as the minimum undeformed thickness of the chip removed from a work surface at a cutting edge under perfect performance of the metal-cutting system (no system deflection). A very fine chip with

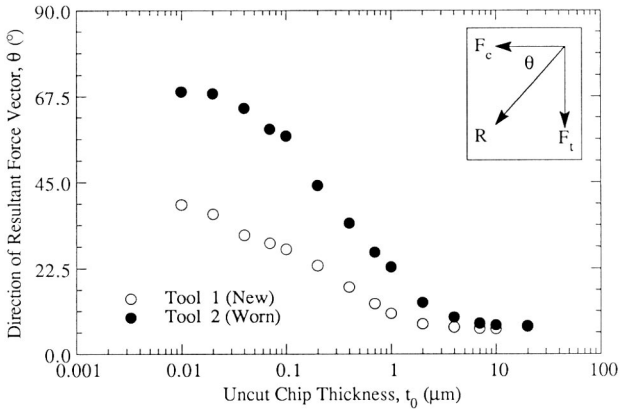

Fig. 2 Direction of resultant force vector for new and worn tools with the same overall tool geometry [20]

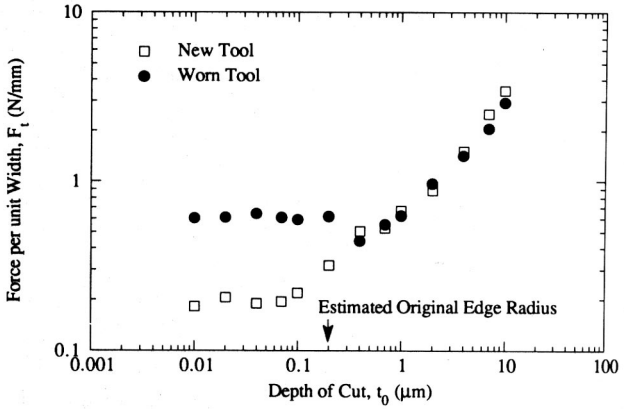

Fig. 3 Effect of tool edge condition on thrust force in orthogonal flycutting of Al 6061-T6 [21]

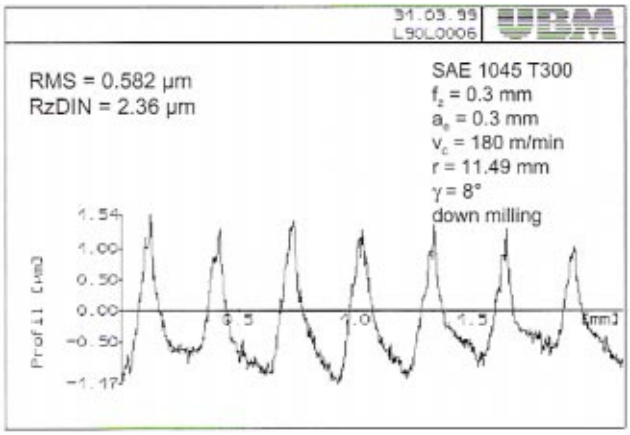

Fig. 5 Measured surface profile [17]

an undeformed thickness on the order of a nanometer, as shown in Fig. 4, was obtained from face turning of electroplated copper by a well-defined diamond tool with an edge radius of around 10 nm. The minimum chip thickness was found to be more strongly affected by the sharpness of the cutting edge than by tool-work interaction. The authors noted that the minimum thickness of cut might be on the order of 1/10 of the cutting edge radius.

The minimum chip thickness effect was also observed in the micromilling process. Weule et al. [17] were the first to point out the existence of the minimum chip thickness and its significant influence on the achievable surface roughness in micro-endmilling. The cutting experiments were carried out using tools of ultrafine tungsten carbide with an edge radius of around 5 μm on SAE 1045 steel tempered at different temperatures. The topography of the machined surface was measured with a laser-based topography measuring device. A sawtoothlike profile was observed as shown in Fig. 5. The authors hypothesized that the minimum chip thickness effect was responsible for the sawtoothlike surface profile. The minimum chip thickness to edge radius ratio for micromachining was estimated to be 0.293 [17], which was much larger than that of nanometric cutting with a much sharper diamond tool (around 1/10 [23]). Figure 6 depicts the formation of the sawtoothlike surface profile considering the minimum chip thickness effect. The authors also noticed that the softer material state (tempered at higher temperatures) caused increased surface roughness. In the ploughing-dominated micromachining process, the increased surface roughness is due to increased ploughing, which is decisively influenced by the minimum chip thickness of the material. Therefore, the authors claimed that the minimum chip thickness was strongly dependent on material properties and suggested that future efforts should be made to understand the interrelationship between the minimum chip thickness and material properties.

Kim et al. [14] performed an experimental study to prove the existence of the minimum chip thickness in micromilling. Full slot cutting was performed on brass using 635 μm micro-endmills with feedrates from 0.188 to 6 μm/flute. The collected chips were examined using a scanning electron microscope (SEM). The SEM pictures were used to estimate the length, width, and thickness of the chips. The chip volumes were then estimated using the trapezoidal numerical integration formula and compared with the nominal chip volume for different feedrates. It was found that for very small feedrates, the measured chip volume is much larger than the nominal chip volume, indicating that a chip is not formed with each pass of the cutting tooth. Further evidence that a chip is not formed with each tooth pass is obtained by examining the distance between the feed marks on the machined surface. For a small feed per tooth, the distance between feed marks was found to be much larger than the feed per tooth, which also indicates that chips do not form with each pass of the tool.

Vogler et al. [18] experimentally studied the effects of minimum chip thickness on the cutting forces in micromilling. The frequency spectrum of the force was found to contain a compo-

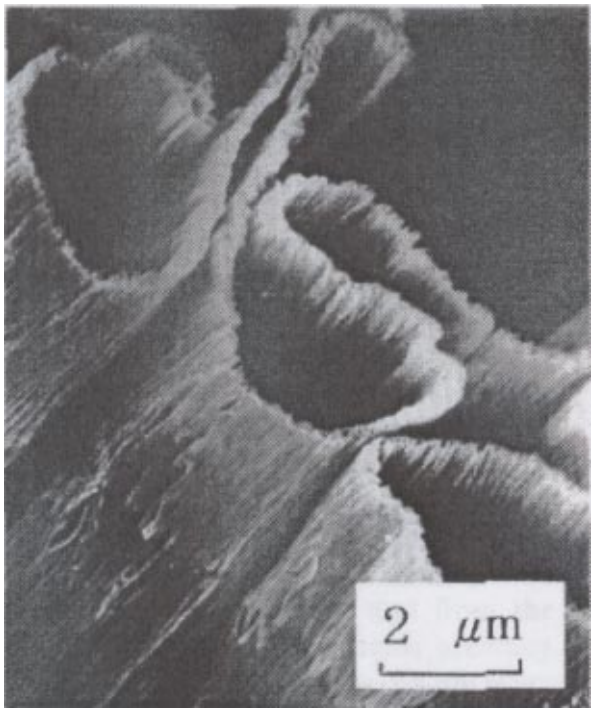

Fig. 4 Chips generated at an uncut chip thickness of 1 nm [23]

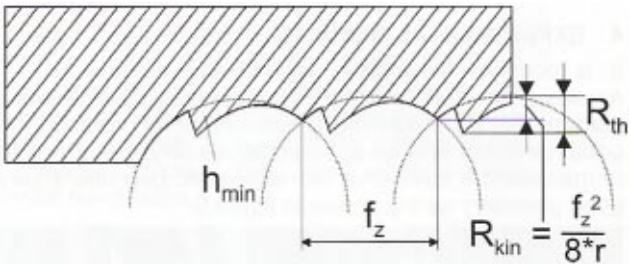

Fig. 6 Theoretical surface profile considering the minimum chip thickness effect [17]

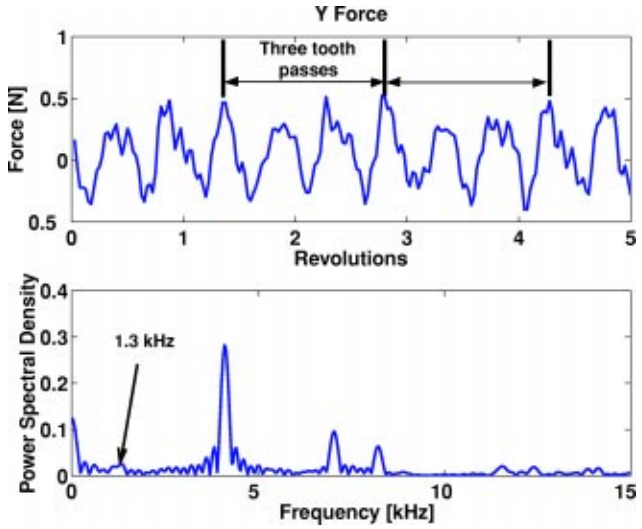

Fig. 7 Experimental Y force (normal to the feed force) and the corresponding power spectrum [14]

nent that is a subharmonic (1/3 for the studied cutting condition) of the tooth passing frequency at a feed rate less than the minimum chip thickness as shown in Fig. 7. This subharmonic frequency component was reflected in the time domain as a repeated pattern every n ($n=3$ for the studied case) tooth passes. Because of the minimum chip thickness effect, when machining at small feedrates, the chip thickness accumulates and the force increases with each tool pass for n tooth passes until the chip thickness is greater than the minimum chip thickness.

Surface Generation and Burr Formation. Surface generation in the micro-endmilling process was studied by Vogler et al. [25]. The surface roughness of the bottom surface of the slot was measured using a Wyko optical profiler. The surface roughness was found to be strongly affected by the tool edge radius. Figure 8 shows that the surface roughness generated by a 5 μm edge radius tool is much larger than that generated by a 2 μm edge radius tool and the machined surface roughness was found to be significantly affected by the feed rate. The authors observed that for the 2 μm edge radius, as the feedrate was reduced to a certain value, the surface roughness started to increase, indicating that an optimal feedrate exists that will produce the smallest surface roughness value. The authors claimed that the existence of the optimal feedrate was due to the tradeoff between the traditional effect of feedmarks as the feed rate is increased and the minimum chip thickness effect resulting in tool passes that do not remove any material as the feed rate is reduced.

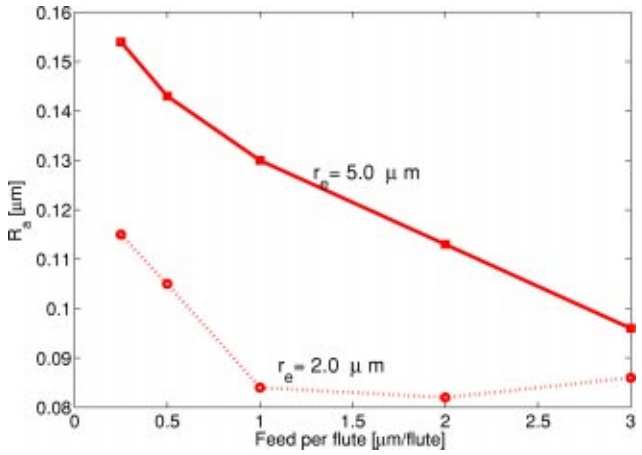

Fig. 8 Effect of tool edge radius on surface roughness for pearlite [25]

Damazo et al. [26] provided a summary of some of the features that were machined by using endmills with a diameter of 200 μm. They reported that burr formation was a major limitation on the minimum wall size that could be machined. The workpiece materials used included aluminum, brass, cast iron, copper, mild steel, and stainless steel. A 25.4 μm thick wall with a 305 μm height was successfully machined.

In Lee and Dornfeld [27], experimental studies on microburr formation in milling aluminum 6061-T6 and copper 110 have been carried out. A range of different chiploads and depths of cut, using 127, 254, and 635 μm tool diameters, were considered. The burr sizes were qualitatively measured using SEM. Different burr formation types in micromilling and conventional milling were discussed. Flag-type, rollover-type, wavy-type, and ragged-type burrs were observed in micromilling aluminum and copper. The rollover-type burr on tool entrance and flag-type burr on tool exit, as shown in Fig. 9, were found to be proportionally bigger than in conventional milling processes considering the ratio of burr size to chip load. The authors attributed this difference to the low cutting speed and large edge radius-to-chipload ratio in micromilling. At low cutting speeds, bending of the chip is more dominant than fracture. As the cutting edge exits from the workpiece, the chip rolls over forming a burr. In addition, the large tool edge radius-to-chipload ratio causes rubbing and compression instead of cutting and generates more burrs. The authors also noted that up-milling produced smaller top burrs than down-milling. As the depth of cut and feed rate increased within the studied range, the burr size was found to increase.

Other Issues: Cutting Temperature, Tool Life, Subsurface Damage, Ductile Mode Machining. The cutting temperature in diamond turning was studied by Iwata et al. [28]. Due to the low cutting energy as well as the high thermal conductivity of both diamond and work materials, such as aluminum and copper, the cutting temperature is quite low in comparison to conventional cutting. However, a small temperature rise in the tool may cause an expansion of the tool shank and, in turn, deterioration in machining accuracy [29].

Tansel and coworkers [30,31] have studied the effect of wear in the micromilling process. They have found that, unlike at conventional sizes, the tool does not gradually wear until it causes undesirable surface effects, but rather the tool breaks quickly as it becomes worn. The fracture of the micro-endmills is due to increased cutting forces with the dulling of the cutting edges causing the stresses to exceed the strength of the small diameter endmills.

In ultraprecision machining, the highly negative effective rake angle and pronounced ploughing cause significant subsurface damage [24]. Lucca et al. [32] experimentally investigated the depth of the plastically deformed layer (subsurface damage) at the workpiece surface in orthogonal ultraprecision machining of both TECU® and fine grain Cu over the range of uncut chip thicknesses of 0.01–10 μm. Two tools with the same nominal geometry but with differing edge geometries were used. Tool edge geometries were characterized by atomic force microscopy, taking into account the AFM cantilever tip radius. The depth of the plastically deformed layer appeared unaffected by the uncut chip thickness but strongly affected by the tool edge radius.

Many researchers have investigated the ductile regime machining of silicon and germanium. Below a critical chip thickness, it was found that plastic deformation rather than brittle fracture of the crystals occurs. It was found that this critical chip thickness increases with more negative rake angles [33,34]. Ichida [35] has determined that increasing the cutting velocity increased the critical chip thickness for ductile machining of silicon. Kaji et al. [36] noticed that the most common way of detecting the presence of

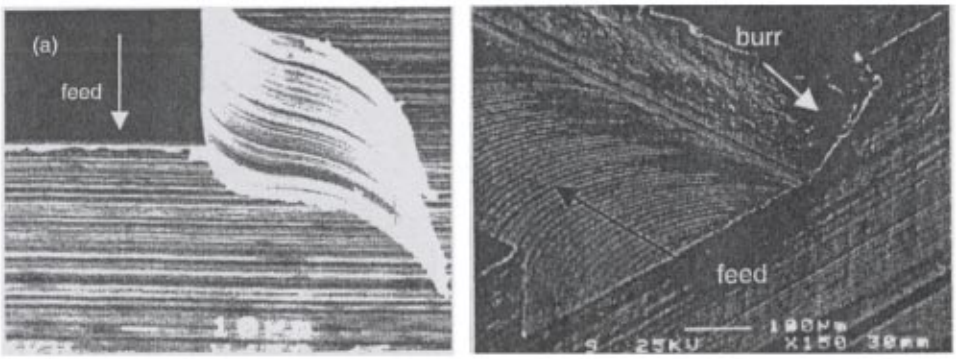

Fig. 9 Burr formation in micromilling: (*a*) flag-type burr on tool exit and (*b*) rollover-type burr on tool entrance [27]

brittle fracture—visual inspection of the freshly cut surface—may not be sufficient because internal cracks develop in the subsurface before cracks appear at the surface.

Arefin et al. [37] carried out a study to investigate the effect of cutting conditions and tool edge radii for nanoscale ductile mode cutting of silicon wafers using single-crystal diamond tools with edge radii ranging from 23 nm to 807 nm. The machined surfaces were examined under SEM. The authors pointed out that two conditions must be satisfied for ductile mode cutting of silicon wafers: the diamond tool edge radius should be smaller than an upper bound (experimentally found to be around 807 nm) and the undeformed chip thickness should be less than the cutting edge radius. Figure 10 shows SEM photographs of the machined surface for different maximum undeformed chip thickness and tool edge radius values. The figure shows only one situation that leads to ductile mode machining.

2.2 Built-up Edge/Elastic-Plastic Deformation. In micromachining, the size effect and the minimum chip thickness phenomenon cause ploughing, and, therefore, the associated material flow pattern and elastic-plastic deformation along the rounded cutting edge plays a dominant role in machining performance. Therefore, it is useful to examine the relevant research that has examined how the material deforms in the vicinity of the cutting edge, e.g., built-up edge formation and the nature and extent of elastic-plastic deformation.

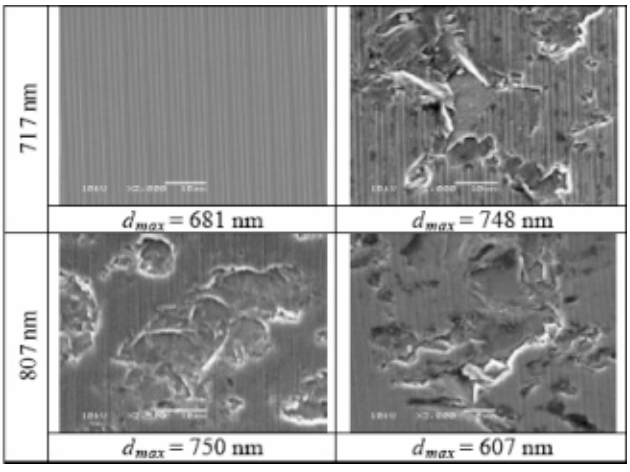

Fig. 10 SEM photographs of machined silicon wafer surfaces for different maximum undeformed chip thickness (d_{max}) and tool edge radius values [37]

Built-up Edge Formation. Many investigators, including Albrecht [38] and Manjunathaiah and Endres [39], assumed the existence of a stagnation point on the cutting edge radius where the workpiece material's tangential velocity vanishes. Other researchers [40,41] believed that there exists a stable build-up, also known as dead metal cap, adhering to the tool, which is stationary while the process attains steady state. Waldorf et al. [42] made a comparison to determine which view of the material flow in the vicinity of the cutting edge is more appropriate in explaining the ploughing force when machining Aluminum 6061-T6. They found out that the model with the assumption of a stable build-up matched the experimental results much better than the model without stable build-up. Kountanya and Endres [43] performed a high magnification visual study of micro-orthogonal cutting while using a blunt tool. They observed the formation of a stable build-up when machining cartridge brass as shown in Fig. 17(*b*). They also observed that the stable build-up was not formed when machining zinc.

Weule et al. [17] conducted fly cutting on SAE 1045 steel under different cutting speeds. They examined the cutting tool edge after each test and found that stable build-up was formed at low cutting speeds, which generated poor surface finish. These studies suggest that the presence or absence of a stable build-up is determined by both the workpiece material and the cutting conditions, especially the cutting speed, which strongly affects the frictional conditions between the workpiece and cutting edge by changing the cutting temperature, strain, and strain rate.

Elastic-Plastic Deformation. Due to the minimum chip thickness effect, the micromachining process is affected by two mechanisms—chip removal and ploughing/rubbing. The extent of ploughing/rubbing and the nature of microdeformation during ploughing/rubbing contributes significantly to burr formation [27] and the corresponding increase in surface roughness [25]. In order to accurately model the micromachining process, it is important to develop methodologies to quantify the elastic-plastic deformation of workpiece material. Scratch testing has been shown to be an effective tool to assess the elastic-plastic deformation of materials. Since the scratching process resembles the micromachining process in that the workpiece material experiences normal pressure and lateral relative motion in both processes, a brief review of scratch testing is helpful in gaining a better understanding of the elastic-plastic deformation in micromachining processes.

Jardret et al. [45] performed instrumented scratch testing on a wide range of materials, from polymers to metals, to understand and characterize the elastic-plastic deformation of materials during scratching. All the experiments were conducted with a Berkovich indenter. The 3D residual scratch morphology was measured using a 3D SURFASCAN topometer. It was observed that the common residual scratch morphology exhibits a groove with

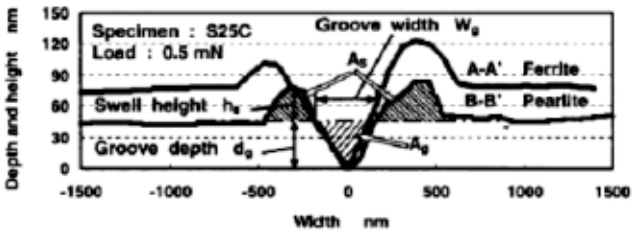

Fig. 11 Cross section profile of scratch groove [44]

two pile-up pads formed by the plastic flow around the indenter. The proportions of the elastic recovery and plastic deformation were computed based on the residual scratch morphology. The authors revealed that the proportion of the plastic deformation increases with the Young's modulus (E) over the hardness (H) ratio E/H for both polymers and metals.

Taniyama et al. [44] also conducted a scratch test on JIS S25C steel with a diamond triangular pyramid indenter under a field emission scanning electron microscope (FE-SEM) in order to reveal the influence of heterogeneity of the workpiece material in the micromachining process. The scratch grooves on different phases were compared. Figure 11 shows the cross section profile of the scratch groove in ferrite and pearlite. It was clearly shown that the scratch groove on pearlite is smaller than that on ferrite. According to the authors, this occurs because pearlite contains lamellar cementite, which is 10 times harder than ferrite. They also discovered that when scratching pearlite, plastic flow was concentrated in the lamellar ferrite rather than lamellar cementite.

2.3 Microstructure Effects. Since the length scale of the crystalline grain size of most commonly used engineering materials, such as steel, aluminum, etc., is between 100 nm and 100 μm and the feature size of micromachined component is of a comparable order, material microstructure effects will play an important role in micromachining. In ultraprecision machining, a typical cutting depth of a few micrometers is common. With such a small depth of cut, chip formation takes place inside the individual grains of a polycrystalline material. The effect of the crystallographic orientation on the mechanism of chip formation [46,47], surface generation [47,48], and the variation of the cutting forces [46,47,49,50] were studied.

Moriwaki et al. [46] conducted in situ machining experiments inside a SEM on single-crystal copper in various cutting direction at depths of cut ranging from 0.1 to 5 μm and a cutting speed of 120 mm/min. They found that the crystallographic orientation affects the chip formation process in terms of the magnitude of the shear angle and the cutting forces. The shear angle was found to reach values as high as 60 deg. Ueda and Iwata [47] investigated the effects of crystallographic orientation on cutting performance during diamond cutting of β-brass. They observed a lamella structure on the free surface of the chip and reported the formation of discontinuous chips in a particular range of crystallographic orientations. They observed shear angle variations from 15 deg to 60 deg with changes in crystallographic orientation. The cutting forces and surface roughness values were also observed to depend on material anisotropy.

To et al. [48] conducted diamond turning of single-crystal aluminum rods with the crystallographic axes normal to ⟨100⟩, ⟨110⟩, and ⟨111⟩ using a diamond tool with a 0 deg rake and a 5 deg clearance angle. The depth of cut varied from 1 to 10 μm. Continuous chip formation was observed under all cutting conditions. They reported that the highest cutting force was produced for the {110} oriented crystals while the lowest for the {111} oriented crystals. They also observed that the best surface finish was obtained in machining crystals with the {100} planes as the cutting planes, whereas the {110} planes would result in the highest surface roughness due to the highest cutting forces and large magnitudes of force variations. According to the authors, the surface roughness was substantially influenced by the crystallographic orientation, but not significantly affected by the depth of cut over the range used in the experiments. Figure 12 shows the effects of the crystallographic orientation and the depth of cut on surface roughness.

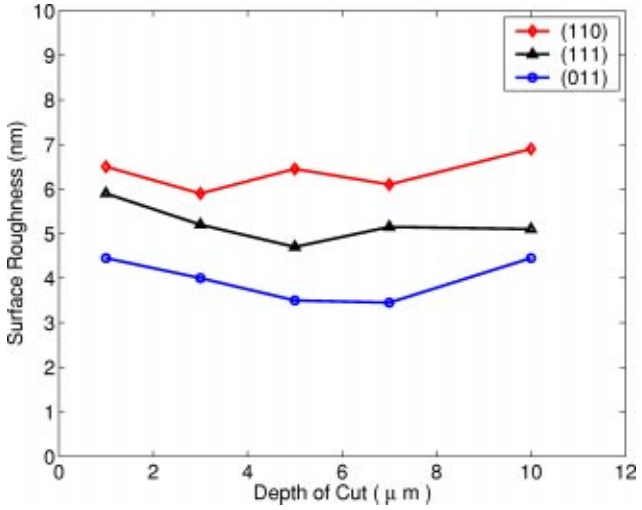

Fig. 12 The effects of the crystallographic orientation and the depth of cut on the surface roughness [48]

In order to gain a better understanding of the effects of a multiphase microstructure on the micromilling process force system, Vogler et al. [18] performed a series of full-slot endmilling tests with 500 μm diam, 2 fluted carbide endmills on both single-phase ferrite and pearlite and multiphase ductile iron. Figure 13 shows the experimental cutting forces and their frequency spectra when machining 50% pearlitic ductile iron at a 30,000 rpm spindle speed and 2 μm/flute feedrate. Besides the energy at the spindle frequency (500 Hz), the tooth-passing frequency (1000 Hz), and their harmonics, there is a significant amount of energy of force variation concentrated around 12 kHz. For a cutting velocity of 48 m/min produced by a 30,000 rpm spindle speed, 12 kHz corresponds to a wavelength of 65.4 μm. This value is extremely close to the average ferrite grain spacing of 70 μm. The cutting force spectra for machining single-phase ferrite and pearlite do not show energy at frequencies above 10 kHz. The presence of the high-frequency components in the ductile iron experiments but

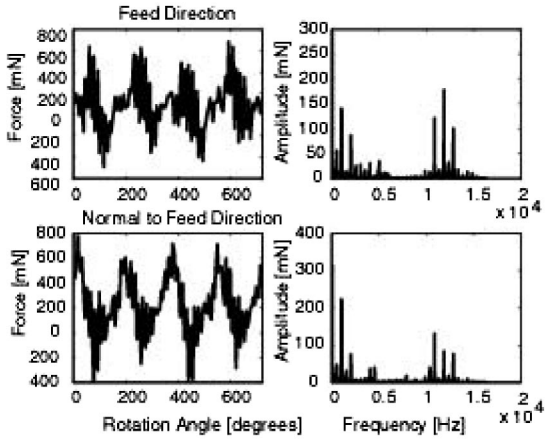

Fig. 13 Experimental cutting forces in micromilling of pearlitic ductile iron [18]

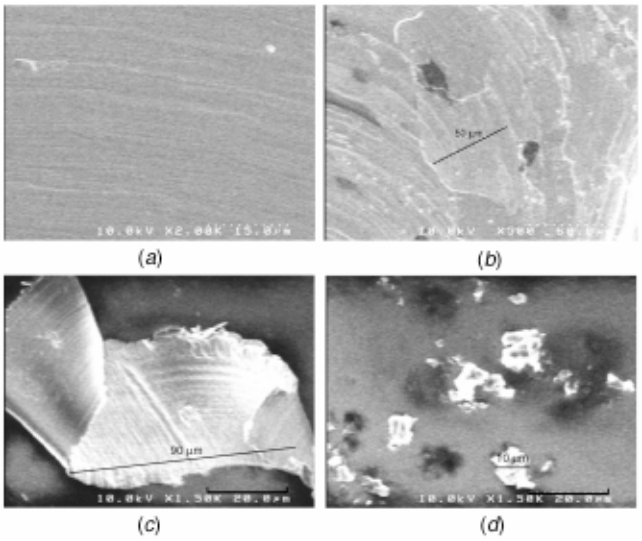

Fig. 14 SEM image of (*a*) ferrite slot floor, (*b*) ferritic ductile iron slot floor, (*c*) fearltie chips, and (*d*) ferritic ductile iron chips [25]

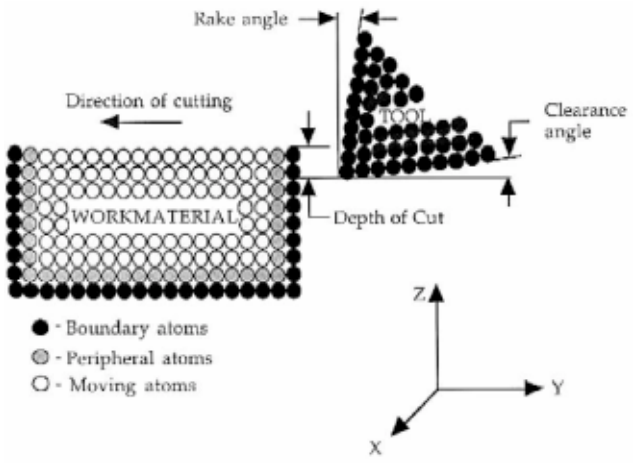

Fig. 15 Schematic of the model used in the MD simulation of nanometric cutting of single-crystal aluminum [56]

not in the ferrite or pearlite tests is further evidence that these high-frequency components are due to the multiphase microstructure.

In addition to the cutting force variation, the effect of the multiphase material microstructure on the surface generation process was also investigated by Vogler et al. [25]. The surface roughness values (Ra values) for multiphase ductile iron are larger than that for the single-phase material over the examined range of cutting conditions. The increased surface roughness was attributed to interrupted chip formation that occurs as the cutting edge moves between the multiple phases. This hypothesis was supported by the frequency spectrum of the surface trace. For ferrite and pearlite, the power spectra are relatively flat and much lower in magnitude than the ductile iron surface spectra. For the ductile iron samples, there are significant peak energies in the spectra around wavelengths of 55 and 67 μm for the ferritic and pearlitic ductile irons, respectively. These wavelengths are near the average phase spacing in the ductile iron specimen of 50 and 70 μm and, therefore, indicate that some phenomena are occurring at the phase boundaries.

To further study the role of phase boundaries, the slot floor was also examined with a SEM, as shown in Fig. 14. For the ferrite slot floor image [Fig. 14(*a*)], the surface appears relatively smooth with no indication of any grain size effects. However, for the ferritic ductile iron [Fig. 14(*b*)], there are clearly some miniature ''burrs'' that have formed at distances that are comparable to the spacing between grain boundaries (white lines in the figure). One possible explanation for this behavior at the phase boundaries is that the chip-formation process is not continuous as the cutting edge moves from one phase to another. As the cutting edge moves between phases, the chip-formation process becomes interrupted as the tool exits a phase at the grain boundary and a burr forms at the phase boundary. To obtain some evidence to test this hypothesis, chips were collected and examined with a SEM as shown in Figure 14. While the fearlite chips [Fig. 14(*c*)] appear continuous, the ferritic ductile iron chips [Fig. 14(*d*)] are highly fragmented, indicating the discontinuous/interrupted nature of the chip-formation process.

3 Modeling Studies

In this section, several key modeling methods for the characterization of micromachining phenomena are discussed. These include molecular dynamics (MD) simulation, the finite element method, the newly emerging field of multiscale simulation modeling, and mechanistic process modeling. MD simulation performs analysis at the atomic level based on the atomic interaction potential and is best suited for nanometric cutting. The underlying theory in the finite element modeling of machining is macroscale continuum mechanics. It is capable of predicting cutting forces, temperatures, stresses, strains, etc., with reasonable accuracy. The multiscale simulation aims at bridging different length scales. The mechanistic modeling approach is directed toward deriving a model that combines a comprehensive characterization of the cutter and cut geometries to relate the process inputs to outputs, while allowing complex material behavior to be characterized through an empirical relation between chiploads and cutting forces calibrated with a small number of experiments.

3.1 Molecular Dynamics (MD) Simulation

Nanometric Cutting Simulation. The application of MD simulation in machining was initiated by a research group at the Lawrence Livermore National Laboratories (LLNL) in the late 1980s [51]. MD simulation was used to study the namometric cutting of copper with a diamond tool [52]. This work led other researchers to explore and extend MD simulation of nanometric cutting to many practical machining applications.

Ikawa et al. [53] studied the 2D nanometric cutting of copper with a diamond tool. They investigated the effect of the edge radius and minimum depth of cut on the chip-formation process and noticed that when the uncut chip thickness is smaller than a fraction of the edge radius, a chip cannot be separated from the workpiece. Therefore, the generated surface is not smooth but is atomically stepwise. Shimada et al. [16] conducted a MD simulation study to determine the ultimate machined surface quality that is attainable in diamond turning of copper with a fine cutting edge under hypothetically perfect machine motion. Based on the analyses, the authors showed that the minimum thickness of cut can be about 1 nm or less, that is, 1/20 to 1/10 of the edge radius of a realistic fine cutting edge available. The ultimate roughness and the depth of the deformed layer of the work surface were found to increase with the increases of the tool edge radius.

Komanduri et al. [54–56] cited a deficiency in the ability to model and measure the scale needed to understand the mechanics of nanometric cutting. To alleviate this problem, they developed a MD model for nanometric cutting. Figure 15 is a schematic of the model used for the MD simulation of nanometric cutting of a single crystal of aluminum to investigate the effect of crystallographic orientation and direction of cutting. While not performing any experimentation, they were able to observe three distinct

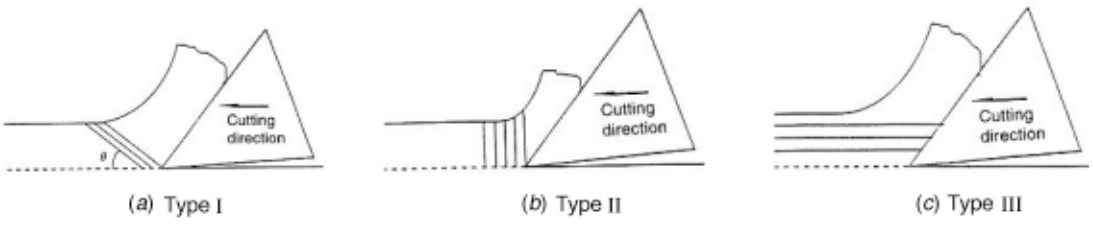

Fig. 16 Three modes of dislocation motion [56]

types (type I, II and III) of dislocation motion when simulating single-crystal aluminum at different orientations (Fig. 16):

i. When machining the [−1 1 0] direction on the (111) plane, chip formation appears to be due to shear and compression ahead of the tool.
ii. When machining the [001] direction on the (110) plane, the dislocations were generated normal to the cutting direction.
iii. When machining the [−1 1 0] direction on the (001) plane, the dislocations were generated parallel to the cutting direction. Of the three types, the cutting force was the smallest for type I and the largest for type II.

MD Simulation in Micromachining. MD simulations were mainly applied to namometric cutting (i.e., the depth of cut in the nanometer range) and not in the general range of micromachining. However the cutting mechanics revealed share some similarity with the cutting mechanics in micromachining. In [57], the authors compared the material flow obtained from MD simulation with experimental results of micromachining conducted by Kountanya and Endres [43]. A clear correlation between the MD-simulated material flow and the actual experimental result was observed. The geometry of the triangular stable build-up and the shear zone predicted by MD simulation are similar to those observed in the experiments as shown in Fig. 17. Further, the MD simulation and slip-line plasticity model developed by Waldorf et al. [40] were combined to predict the cutting forces for different depth of cut over edge radius ratios. The MD simulated results were used to extract the geometric parameters, such as shear angle, prow angle of the slip-line field. The predicted cutting forces were normalized and compared to micromachining experiment results. There is a strong correlation in the trend of the normalized forces, with both data showing the existence of a local maximum in the thrust force with respect to the uncut chip thickness.

3.2 Finite Element Method

Edge Radius Effect. Moriwaki et al. [58] developed a finite element model of the machining process capable of modeling the thermomechanical properties of the workpiece during cutting with an edge radiused tool. The model developed was used to analyze the stress, strain, material flow, flow of the cutting heat, and temperature distribution within both the workpiece and the tool in orthogonal micro-machining of copper. They showed that the specific cutting and thrust energies increased as the ratio of the tool edge radius to the depth of cut decreased. The simulation results of the stress distribution revealed that the affected zone within the workpiece was expanded as the ratio of the edge radius to the depth of cut was increased. The predicted cutting temperature was found to increase with an increase in cutting speed. The cutting temperature is about 270 K higher than the mean temperature of the workpiece when copper is cut at a cutting speed of 4.3 m/s and a depth of cut of 1 μm. The temperature gradient in the workpiece becomes larger in front of the cutting edge due to the material flow relative to the cutting tool.

Size Effect. In addition to the edge radius, Dinesh et al. [59] suggested that the strain gradient could also be a major cause of the size effect in micromachining since the strain gradient in machining is very intense. Liu and Melkote [60] presented a strain gradient-based finite element model for orthogonal cutting to predict the size effect in microcutting. The strain gradient strengthening leads to a higher effective stress in the deformation zones, which, in turn, results in a higher specific cutting energy with decreased chip thickness. The contours of the effective stresses, presented in Fig. 18, show that the maximum effective stress is higher with strain gradient effects than without. Figure 19 compares the predicted specific cutting energy versus the uncut chip thickness with and without considering strain gradient effects. The specific cutting energy predicted by the finite element model with

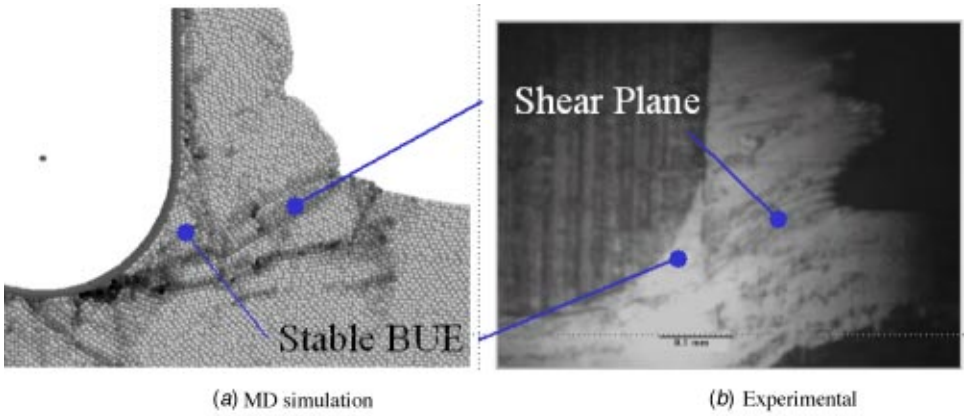

Fig. 17 Material flow near a rounded cutting edge [57]

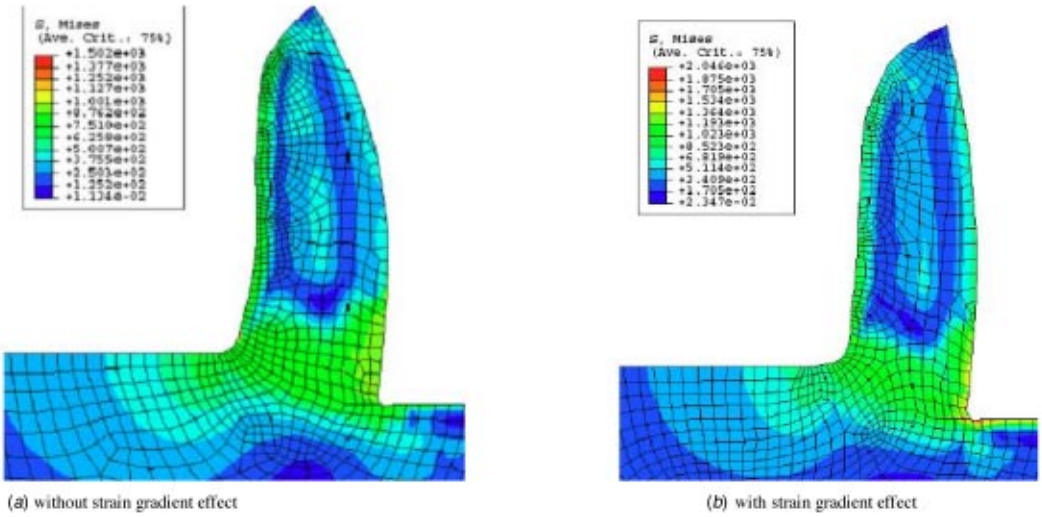

Fig. 18 Effective stress contours [60]

strain gradient effects increases in a nonlinear fashion by nearly 40% when the uncut chip thickness decreases from 70 to 20 μm. The increasing trend of the specific cutting energy, as the uncut chip thickness decreases, matches well with the experiment results given in Kopalinsky and Oxley [61].

Microstructure-Level Modeling. Chuzhoy et al. [62] developed a FE model for the orthogonal machining of ductile iron. This is the first machining paper to explicitly model the various phases of the iron—ferrite and pearlite with different constitutive models to account for the heterogeneity of the workpiece material. The model is capable of computing stress, strain, temperature and damage. It can also predict the size of fracture and decohesion zones for ductile iron machining. The work shows the potential for capturing the damage between phases in the machining of multiphase ductile iron. Vogler et al. [25] used Chuzhoy's model to determine the minimum chip thickness values for pearlite and ferrite, which explicitly account for the effects of the material's properties on the minimum chip thickness. The ductility of the material was found to have the most significant influence on the minimum chip thickness. The more ductile ferrite was found to have a larger minimum chip thickness than pearlite.

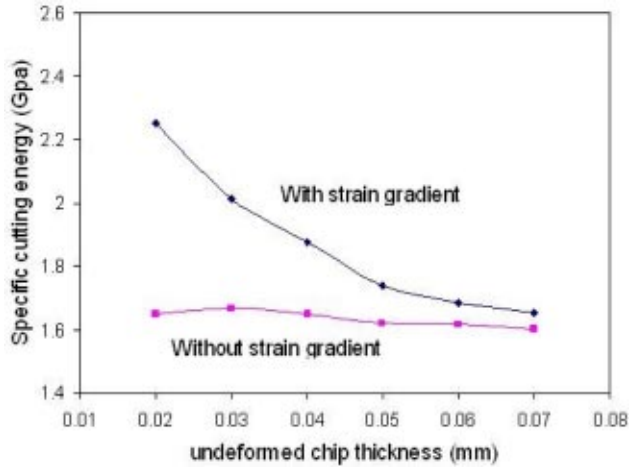

Fig. 19 Variation of specific cutting energy with undeformed chip thickness [60]

3.3 Multiscale Simulation. For the purpose of investigating the differences between the mechanics of nanometric cutting and the mechanics of cutting at the macroscale, Inamura et al. [63] introduced a method of transformation from an atomic MD model of nanometric cutting to an equivalent continuum FEM model to evaluate the stress and strain distribution in nanometric cutting. The results showed that the stress/strain distributions during nanometric cutting could not be explained by the theory of plasticity at the macroscale. The length scale of micromachining falls within nanometric cutting and macromachining. The mechanics of micromachining inherently has the characteristics of both. The mechanics at different length scales interact strongly to produce the observed behavior. For instance, microburr formation at the phase boundaries may be best described at the nanoscale with MD simulation, while the stress and strain distribution within a grain or in the far-field of the workpiece may be accurately represented with macroscale continuum mechanics via FE modeling. The newly emerging field of multiscale simulation which aims at developing methodologies to couple different length scales will provide insight into the development of micromachining process models.

In [64,65], Abraham, Broughton, and their co-workers developed a methodology to couple different size scales from continuum (macroscale) to statistical (atomic scale) to quantum mechanics (electron scale) by implementing an algorithm that is capable of handshaking between FEM, MD, and semi-empirical tight binding. The methodology was successfully applied to study crack propagation in silicon. Lidorikis et al. [66] used a hybrid MD and FEM simulation approach to study stress distributions in silicon/silicon-nitride nanopixels. The hybrid approach provides an atomistic description near the interface and a continuum description deep into the substrate, increasing the accessible length scales and greatly reducing the computational cost. Zhigilei [67] presented a study using multiscale simulation to investigate the laser ablation phenomenon. The multiscale approach addresses different processes involved in laser ablation with appropriate resolutions and, at the same time, accounts for the interrelations between the processes. While to date, multiscale simulation has not been specifically applied to micromachining, it shows considerable promise for dealing with the multiplicity of issues that arise over this and neighboring size scales.

3.4 Mechanistic Modeling

Microstructure Effect. A mechanistic model for the microendmilling process has been developed by Vogler et al. [18] that

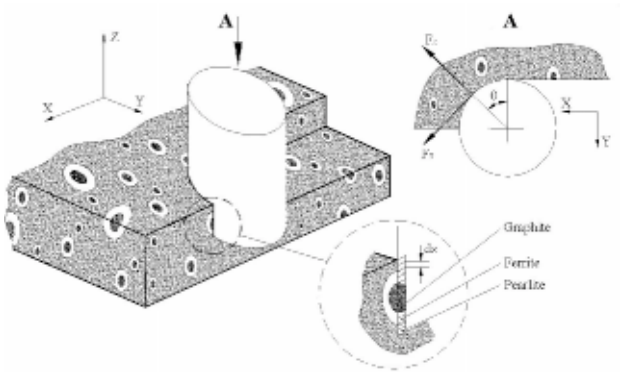

Fig. 20 Endmilling of ductile iron workpiece [18]

utilized a mapping technique to represent the microstructure of the different phases of multiphase materials in determining the magnitude and variation of the cutting forces. Figure 20 illustrates the process of endmilling multiphase ductile iron. The model recognizes at any instant in the cut, exactly what part of the cutting-edge engagement is in each phase of the multiphase material. The model is validated by using calibrated specific cutting force coefficients from pearlite and ferrite, the major components of ductile iron, to predict the cutting force magnitude and variation in micro-endmilling of ductile iron.

The model was shown to be capable of capturing the high frequency variation of the cutting forces that was observed in experiments (shown earlier in Fig. 13) but can not be explained by the kinematics of the process when micromilling ductile iron. The simulation studies show that the frequency of the variation can be attributed to the spacing of the secondary phase and that the magnitude of the variation is determined by the size of the secondary phase particles.

Edge Radius Effect. Kim and Kim [68] developed an orthogonal cutting force model, which includes the cutting edge radius effect and the elastic recovery along the clearance face of the cutter. Four regions of stresses are considered in developing the round edge cutting model (RECM): the normal and friction stresses on the rake face, the normal and friction stresses on the clearance face of the tool due to the elastic recovery of the workpiece, the friction and normal stresses on the round edge, and the effect of the negative rake angle on the shearing geometry. To compute the normal stresses on the edge radius, a work-hardening model is used to model the workpiece material. Model predictions are compared with the experimental results from Lucca et al. [19]. The RECM is shown to predict the observed trends much more accurately than Merchant's sharp edge cutting model.

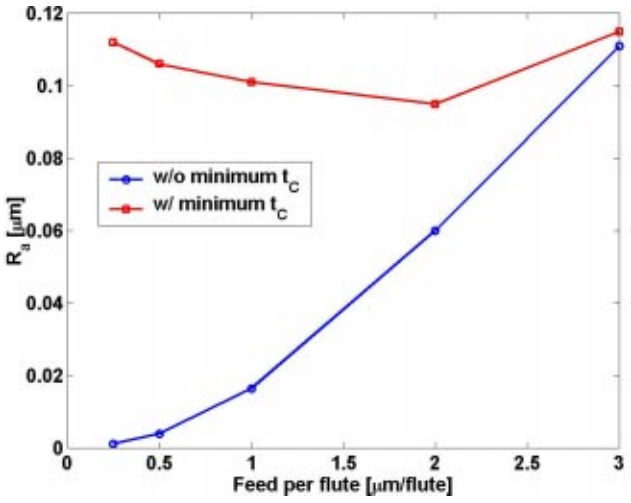

Fig. 21 Effect of minimum chip thickness on surface roughness [25]

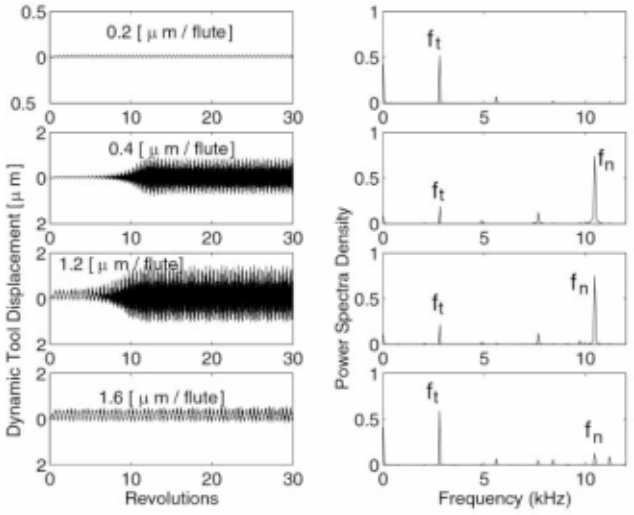

Fig. 22 Tool vibration histories and frequency spectra for machining pearlite at different feed rate [71]

In order to explicitly account for the cutting edge radius, Vogler et al. [69] extended a previously developed micromilling force model [18] by incorporating the minimum chip thickness effect, on the chip thickness modulation. The cutting forces originating from two mechanisms—chip removal and ploughing/rubbing—were computed separately using slip-line plasticity and interference volume, respectively. The experimental observed subharmonic of the tooth passing frequency in the power spectrum as shown earlier in Fig. 7 when machining at a small feedrate was accurately predicted. It was also noted that the predicted cutting force signal contained a repeated pattern every *n* tooth passes similar to the experimental data shown earlier in Fig. 7, which provide an additional evidence of the minimum chip thickness phenomena in micro-machining.

Size Effect. Joshi and Melkote [70] made an attempt at explaining the size effect in the Primary Deformation Zone (PDZ) of an orthogonal cutting process by developing a strain gradient plasticity-based model. Considering a parallel-sided configuration of the PDZ, models are formulated for the strain gradient, density of geometrically necessary dislocations, shear strength, and the specific shear energy. The analysis shows that for deformation in the PDZ, the length of the shear plane represents the material length scale. The model also provides an estimate of the lower bound on the size effect observed in the specific shear energy. Trends in the predicted specific shear energy match well with experimental values obtained from the literature.

Surface Generation. Vogler et al. [25] developed a process model of micro-endmilling for the prediction of the surface roughness for the slot floor centerline and cutting forces. The model explicitly accounted for the effect of finite edge radius by incorporating the minimum chip thickness concept. The minimum chip thickness values were found through finite element simulations for the ferrite and pearlite materials. The model is shown to accurately predict the surface roughness for single-phase materials, viz., ferrite and pearlite. Two phenomena were found to combine to generate an optimal feed rate for the surface generation of single-phase materials, the geometric effect of the tool and process geometry and the minimum chip thickness effect. Figure 21

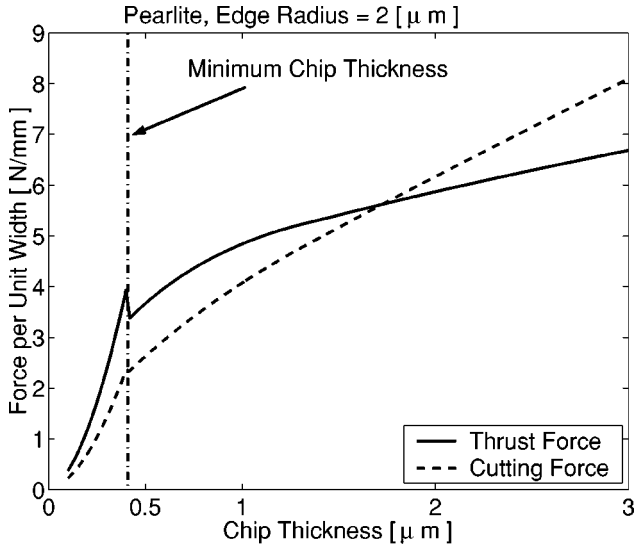

Fig. 23 Chipload/force relationship for pearlite [71]

shows the effect of the minimum chip thickness on the surface roughness. The effect of the minimum chip thickness is dominant at lower values of the feed rate.

Dynamic Modeling. Liu et al. [71] developed a dynamic cutting force and vibration model of the micro-endmilling process that accounts for the dynamics of the micro-endmill, influences of the stable built-up edge, and the effects of minimum chip thickness, elastic recovery, and the elastic-plastic nature in ploughing/rubbing. Using the model, the authors studied the effects of the minimum chip thickness on the cutting forces and vibrations as well as the stability of the micro-endmilling process. A salient feature of stability in micromilling, that differentiates it from the stability of conventional milling, is that stability becomes sensitive to the feed rate, resulting in a low feed rate instability phenomenon. Figure 22 shows the predicted tool vibration histories and the frequency spectra for machining pearlite using a 2 μm edge radius micro-endmill with a 50 μm depth of cut at different federates. It is clearly seen that as the feed rate increases from 0.2 to 0.4 μm/flute, the vibration level dramatically increases and the frequency spectrum contains significant energy at the tool's natural frequency (f_n) of 10.4 kHz, indicating an unstable cut. On the other hand, as the feed rate increases from 1.2 to 1.6 μm/flute, the vibration level decreases and the frequency spectrum becomes dominated by the tooth passing frequency (f_t) of 2.8 kHz, suggesting that the process changes from unstable back to stable.

The authors attributed the feed rate-dependent stability to the highly nonlinear and discontinuous chipload/force relationship shown in Fig. 23. First, the rate of increase for both the cutting force and thrust force is much higher for ploughing/rubbing (when the chip thickness is smaller than the minimum chip thickness) than for the chip formation process (when the chip thickness is larger than the minimum chip thickness). Further, a local maximum of the thrust force at the minimum chip thickness, due to the transition between ploughing and shearing, was clearly shown, which is in agreement with the experimental observations presented in [57].

4 Conclusions

This paper has provided a review of the literature of the last 10–15 years that collectively is defining the science base required to explain phenomena unique to machining (cutting processes) at the microscale. Based on this assessment of the current state of the science, some observations concerning past work and future needs are offered:

1. Although recent studies have begun to focus more on modeling tools and methods for micromachining process characterization, the majority of the work to date has been experimental in nature.
2. There exists a body of work, mostly experimental in nature, in the area of ultraprecision machining that is helping to explain a number of observed phenomena in the world of micromachining.
3. The current state of the art of cutting tool manufacturing at the microscale has a significant impact on the mechanics of the process. More attention to this area will be important to the economics of machining at this size-scale.
4. Little work can be found that deals with the thermal aspects of machining at the microscale. This is an area where more research is needed.
5. The dynamics of micromachining, including process stability issues and vibrations, have not been examined in depth to date.
6. The emerging field of multiscale modeling will likely play an important role in the characterization of machining at reduced size scales, particularly in explaining phenomenological effects across the nano-micro-meso continuum.
7. More work is needed to develop improved methods for the estimation of minimum chip thickness values for a wide range of materials.
8. Because surface-to-volume ratios increase as the size scale reduces, more attention to surface generation and phenomena that influence the surface character should be forthcoming.
9. Subsurface damage is also an important issue of research due to the significant ploughing in micromachining.

Acknowledgments

The authors gratefully acknowledge the financial support of the University of Illinois at Urbana-Champaign National Science Foundation Nano-CEMMS Center under NSF Grant No. 0328162, and the financial support of the National Science Foundation through Grant No. DMII01-14717.

References

[1] Friedrich, C. R., and Kang, S. D., 1994, "Micro Heat Exchangers Fabricated by Diamond Machining," Precision Eng., **16**, pp. 56–59.
[2] Adams, D. P., Vasile, M. J., and Krishnan, A. S. M., 2000, "Microgrooving and Microthreading Tools for Fabricating Curvilinear Features," Precision Eng., **24**, pp. 347–356.
[3] Adams, D. P., Vasile, M. J., Benavides, G., and Campbell, A. N., 2001, "Micromilling of Metal Alloys With Focused Ion Beam-Fabricated Tools," Precision Eng., **25**, pp. 107–113.
[4] Egashira, K., Mizutani, K., and Nagao, T., 2002, "Ultrasonic Vibration Drilling of Microholes in Glass," CIRP Ann., **51**, pp. 339–342.
[5] Egashira, K., and Mizutani, K., 2002, "Micro-Drilling of Monocrystalline Silicon Using a Cutting Tool," Precision Engineering, **26**, pp. 263–268.
[6] Schaller, Th., Bohn, L., Mayer, J., and Schubert, K., 1999, "Microstructure Grooves With a Width of Less Than 50 μm Cut With Ground Hard Metal Micro End Mills," Precision Eng., **23**, pp. 229–235.
[7] Takeuchi, Y., Sawada, K., and Sata, T., 1996, "Ultraprecision 3D Micromachining of Glass," CIRP Ann., **45**, pp. 401–404.
[8] Friedrich, C. R., and Vasile, M. J., 1996, "Development of the Micromilling Process for High-Aspect-Ratio Microstructures," J. Microelectromech. Syst., **5**, pp. 33–38.
[9] Shoji, S., and Esashi, M., 1994, "Microflow Devices and Systems," J. Micromech. Microeng., **4**, pp. 157–171.
[10] Suzuki, H., Ohya, N., Kawahara, N., Yokoi, M., Ohyanagi, S., Kurahashi, T., and Hattori, T., 1995, "Shell-Body Fabrication for Micromachines," J. Micromech. Microeng., **5**, pp. 36–40.
[11] Tritschler, H., Schmidt, J., Spath, D., Elsner, J., and Huntrup, V., 2002, "Requirements of an Industrially Applicable Microcutting Process for Steel Microstructures," Microsys. Technol., **8**, pp. 402–408.
[12] Fang, N., 2003, "Slip-Line Modeling of Machining With a Rounded-Edge Tool—Part II: Analysis of the Size Effect and the Shear Strain-Rate," J. Mech. Phys. Solids, **51**, pp. 743–762.
[13] Manjunathaiah, J., and Endres, W. J., 2000, "A Study of Apparent Negative Rake Angle and its Effects on Shear Angle During Orthogonal Cutting With Edge-Radiused Tools.," Trans. NAMRI/SME, **28**, pp. 197–202.
[14] Kim, C. J., Bono, M., and Ni, J., 2002, "Experimental Analysis of Chip For-

mation in Micro-Milling,'' Trans. NAMRI/SME, **30**, pp. 1–8.
[15] Yuan, Z. J., Zhou, M., and Dong, S., 1996, ''Effect of Diamond Tool Sharpness on Minimum Cutting Thickness and Cutting Surface Integrity in Ultraprecision Machining,'' J. Mater. Process. Technol., **62**, pp. 327–330.
[16] Shimada, S., Ikawa, N., Tanaka, H., Ohmori, G., Uchikoshi, J., and Yoshinaga, H., 1993, ''Feasibility Study on Ultimate Accuracy in Microcutting Using Molecular Dynamics Simulation,'' CIRP Ann., **42**, pp. 91–94.
[17] Weule, H., Huntrup, V., and Tritschle, H., 2001, ''Micro-Cutting of Steel to Meet New Requirements in Miniaturization,'' CIRP Ann., **50**, pp. 61–64.
[18] Vogler, M. P., DeVor, R. E., and Kapoor, S. G., 2001, ''Microstructure-Level Force Prediction Model for Micro-Milling of Multi-Phase Materials,'' Proc. ASME Manufacturing Engineering Division (MED-vol. 12) ASME International Mechanical Engineering Congress and Exposition, NY, pp. 3–10.
[19] Lucca, D. A., Rhorer, R. L., and Komanduri, R., 1991, ''Energy Dissipation in the Ultraprecision Machining of Copper,'' CIRP Ann., **40**, pp. 69–72.
[20] Lucca, D. A., and Seo, Y. W., 1993, ''Effect of Tool Edge Geometry on Energy Dissipation in Ultraprecision Machining,'' CIRP Ann., **42**, pp. 83–86.
[21] Lucca, D. A., Seo, Y. W., and Rhorer, R. L., 1994, ''Energy Dissipation and Tool-Workpiece Contact in Ultra-Precision Machining,'' STLE Tribol. Trans., **37**, pp. 651–655.
[22] Taminiau, D. A., and Dautzenberg, J. H., 1991, ''Bluntness of the Tool and Process Forces in High-Precision Cutting,'' CIRP Ann., **40**, pp. 65–68.
[23] Ikawa, N., Shimada, S., Tanaka, H., and Ohmori, G., 1991, ''Atomistic Analysis of Nanometric Chip Removal as Affected by Tool-Work Interaction in Diamond Turning,'' CIRP Ann., **40**, pp. 551–554.
[24] Ikawa, N., Donaldson, R. R., Komanduri, R., Koenig, W., Aachen, T. H., McKeown, P. A., Moriwaki, T., and Stowers, I. F., 1991, ''Ultraprecision Metal Cutting, The Past, the Present, and the Future,'' CIRP Ann., **40**, pp. 587–594.
[25] Vogler, M. P., DeVor, R. E., and Kapoor, S. G., 2004, ''On the Modeling and Analysis of Machining Performance in Micro-endmilling, Part I: Surface Generation,'' ASME J. Manuf. Sci. Eng., **126**(4), pp. 684–693.
[26] Damazo, B. N., Davies, M. A., Dutterer, B. S., and Kennedy, M. D., 1999, ''A Summary of Micro-Milling Studies,'' *Proc. of 1st International Conference and General Meeting of the European Society for Precision Engineering and Nanotechnology*, Bremen, Germany, European Society of Precision Engineering, pp. 322–325.
[27] Lee, K., and Dornfeld, D. A., 2002, ''An Experimental Study on Burr Formation in Micro Milling Aluminum and Copper,'' Trans. NAMRI/SME, **30**, pp. 1–8.
[28] Iwata, K., Moriwaki, T., and Okuda, K., 1987, ''A Study of Cutting Temperature in Ultra-high Precision Diamond Cutting of Copper,'' Transaction of the NAMRI/SME, **15**, pp. 510–515.
[29] Moriwaki, T., Horiuchi, A., and Okuda, K., 1990, ''Effect of Cutting Heat on Machining Accuracy in Ultra-Precision Diamond Turning,'' CIRP Ann., **39**, pp. 81–84.
[30] Tansel, I. N., Arkan, T. T., Bao, W. Y., Mahendrakar, N., Shisler, B., Smith, D., and McCool, M., 2000, ''Tool Wear Estimation in Micro-Machining. Part I: Tool Usage-Cutting Force Relationship,'' Int. J. Mach. Tool Des. Res., **40**, pp. 599–608.
[31] Tansel, I., Rodriguez, O., Trujillo, M., Paz, E., and Li, W., 1998, ''Micro-End-Milling—I. Wear and Breakage,'' Int. J. Mach. Tool Des. Res., **38**, pp. 1419–1436.
[32] Lucca, D. A., Seo, Y. W., Rhorer, R. L., and Donaldson, R. R., 1994, ''Aspects of Surface Generation in Orthogonal Ultraprecision Machining,'' CIRP Ann., **43**, pp. 43–46.
[33] Blake, P. N., and Scattergood, R. O., 1990, ''Ductile-Regime Machining of Germanium and Silicon,'' J. Am. Ceram. Soc., **73**, pp. 949–957.
[34] Li, D., Dong, S., Zhao, Y., and Zhou, M., 1999, ''The Influence of Rake of Diamond Tool on the Machined Surface of Brittle Materials With Finite Element Analysis,'' *Proc. of 1st International Conference and General Meeting of the European Society for Precision Engineering and Nanotechnology*, Bremen, Germany, European Society of Precision Engineering, pp. 338–341.
[35] Ichida, Y., 1999, ''Ductile Mode Maching of Single Crystal Silicon Using a Single Point Diamond Tool,'' *Proc. of 1st International Conference and General Meeting of the European Society for Precision Engineering and Nanotechnology*, Bremen, Germany, European Society of Precision Engineering, pp. 330–333.
[36] Kaji, S., Goto, T., Sumomogi, T., and Nakamura, M., 1999, ''The Study of Ductile-Brittle Transition on Micro-Cutting of Single Crystal Silicon,'' *Proc. Annual Meeting of the ASPE*, Vol. 20, pp. 107–110.
[37] Arefin, S., Liu, K., Li, X. P., and Rahman, M., 2004, ''Cutting Conditions and Tool Edge Radius for Nanoscale Ductile Cutting of Silicon Wafer,'' *Proc. of 2004 Japan-USA Symposium on Flexible Automation*, CD, Paper No. UL_031.
[38] Albrecht, P., 1960, ''New Developments in Theory of Metal-Cutting Process—1. Ploughing Process in Metal Cutting,'' ASME J. Eng. Ind., **82**, pp. 348–358.
[39] Manjunathaiah, J., and Endres, W. J., 2000, ''A New Model and Analysis of Orthogonal Machining With an Edge-Radiused Tool,'' ASME J. Manuf. Sci. Eng., **122**, pp. 384–390.
[40] Waldorf, D. J., DeVor, R. E., and Kapoor, S. G., 1998, ''Slip-Line Field for Ploughing During Orthogonal Cutting,'' ASME J. Manuf. Sci. Eng., **120**, pp. 693–698.
[41] Zhang, H. T., Liu, P. D., and Hu, R. S., 1991, ''A Three-Cap Model and Solution of Shear Angle in Orthogonal Machining,'' Wear, **143**, pp. 29–43.
[42] Waldorf, D. J., DeVor, R. E., and Kapoor, S. G., 1999, ''An Evaluation of Ploughing Models for Orthogonal Machining,'' ASME J. Manuf. Sci. Eng., **121**, pp. 550–558.
[43] Kountanya, R. K., and Endres, W. J., 2001, ''A High-Magnification Experimental Study of Orthogonal Cutting With Edge-Honed Tools,'' ASME Proceedings of the ASME Manufacturing Engineering Division (MED-Vol. 12), 2001 ASME International Mechanical Engineering Congress and Exposition, N.Y., pp. 157–164.
[44] Taniyama, H., Eda, H., Zhou, L., Shimizu, J., and Sato, J., 2003, ''Experimental Investigation of Micro Scratching on the Two-Phase Steel: Plastic Flow Mechanisms of the Ferrite and Cementite Phases,'' Key Eng. Mater., **238-239**, pp. 15–18.
[45] Jardret, V., Zahouani, H., Loubet, J. L., and Mathia, T. G., 1998, ''Understanding and Quantification of Elastic and Plastic Deformation During a Scratch Test,'' Wear, **218**, pp. 8–14.
[46] Moriwaki, T., Sugimura, N., Manabe, K., and Iwata, K., 1991, ''A Study on Orthogonal Micromachining of Single Crystal Copper,'' Transaction of the NAMRI/SME, **19**, pp. 177–183.
[47] Ueda, K., and Iwata, K., 1980, ''Chip Formation Mechanism in Single Crystal Cuting of Beta-Brass,'' CIRP Ann., **29**, pp. 65–68.
[48] To, S., Lee, W. B., and Chan, C. Y., 1997, ''Ultraprecision Diamond Turning of Aluminum Single Crystals,'' J. Mater. Process. Technol., **63**, pp. 157–162.
[49] Lee, W. B., To, S., and Cheung, C. F., 2000, ''Effect of Crystallographic Orientation in Diamond Turning of Copper Single Crystals,'' Scr. Mater., **42**, pp. 937–945.
[50] Patten, J., Mundy, P., Fang, N., and Domblesky, J., 2004, ''Advanced Machining of Alternative Materials—Part A: Cutting Mechanics,'' [SME International Manufacturing Technology Summit], Dearborn, MI, Proc. of 1st Annual Manufacturing Technology Summit Conference, 2004, Dearborn, MI, pp. 1–11.
[51] Belak, J. and Stowers, I. F., 1990, ''A Molecular Dynamics Model of the Orthogonal Cutting Process,'' *Proc. of ASPE Annual Conference*, Oct. 13–18, 1991, pp. 100–104.
[52] Belak, J., Lucca, D. A., Komanduri, R., Rhoerer, R. L., Moriwaki, K., Okuda, S., Ikawa, N., Shimada, S., Tanaka, H., Dow, T. A., Drescher, J. D., and Stowers, I. F., 1991, ''Molecular Dynamics Simulation of the Chip Formation Process in Single Crystal Copper and Comparison With Experimental Data,'' *Proc. ASPE Annual Conference*, Oct. 13–18, pp. 100–109.
[53] Ikawa, N., Shimada, S., and Tanaka, H., 1992, ''Minimum Thickness of Cut in Micromachining,'' Nanotechnology, **3**, pp. 6–9.
[54] Komanduri, R., Chandrasekaran, N., and Raff, L. M., 1998, ''Effect of Tool Geometry in Nanometric Cutting: A Molecular Dynamics Simulation Approach,'' Wear, **219**, pp. 84–97.
[55] Komanduri, R., Chandrasekaran, N., and Raff, L. M., 1999, ''Orientation Effects in Nanometric Cutting of Single Crystal Materials: An MD Simulation Approach,'' CIRP Ann., **48**, pp. 67–72.
[56] Komanduri, R., Chandrasekaran, N., and Raff, L. M., 2000, ''M.D. Simulation of Nanometric Cutting of Single Crystal Aluminum-Effect of Crystal Orientation and Direction of Cutting,'' Wear, **242**, pp. 60–88.
[57] Liu, X., Vogler, M. P., Kapoor, S. G., DeVor, R. E., Ehmann, K. F., Mayor, R., Kim Changju, and Ni, J., 2004, ''Micro-Endmilling With Meso-Machine-Tool System,'' *NSF Design, Service and Manufacturing Grantees and Research Conference Proc.*, Dallas, TX.
[58] Moriwaki, T., Sugimura, N., and Luan, S., 1993, ''Combined Stress, Material Flow and Heat Analysis of Orthogonal Micromachining of Copper,'' CIRP Ann., **42**, pp. 75–78.
[59] Dinesh, D., Swaminathan, S., Chandrasekar, S., and Farris, T. N., 2001, ''An Intrinsic Size-Effect in Machining Due to the Strain Gradient,'' Proc. ASME Manufacturing Engineering Division (MED-vol. **12**), ASME International Mechanical Engineering Congress and Exposition, NY, pp. 197–204.
[60] Liu, K., and Melkote, S. N., 2004, ''A Strain Gradient Based Finite Element Model for Micro/Meso-Scale Orthogonal Cutting Process,'' *Proc. of 2004 Japan-USA Symposium on Flexible Automation*, Denver, CO, Paper No. UL_048.
[61] Kopalinsky, E. M., and Oxley, P. L. B., 1984, *Size Effect in Metal Removal Processes*, Inst of Physics, Bristol, pp. 389–396.
[62] Chuzhoy, L., DeVor, R. E., Kapoor, S. G., and Bammann, D. J., 2001, ''Microstructure-Level Modeling of Ductile Iron Machining,'' Proc. ASME Manufacturing Engineering Division (MED-Vol. **12**), 2001 ASME International Mechanical Engineering Congress and Exposition, NY, pp. 125–134.
[63] Inamura, T., Takezawa, N., Kumai, Y., and Sata, T., 1994, ''On a Possible Mechanism of Shear Deformation in Nanoscale Cutting,'' CIRP Ann., **43**, pp. 47–50.
[64] Abraham, F. F., Broughton, J. Q., Bernstein, N., and Kaxiras, E., 1998, ''Spanning the Length Scales in Dynamic Simulation,'' Comput. Phys., **12**, pp. 538–546.
[65] Broughton, J. Q., Abraham, F. F., Bernstein, N., and Kaxiras, E., 1999, ''Concurrent Coupling of Length Scales: Methodology and Application,'' Phys. Rev. B, **60**, pp. 2391–2403.
[66] Lidorikis, E., Bachlechner, M. E., Kalia, R. K., Voyiadjis, G. Z., Nakano, A., and Vashishta, P., 2001, *Coupling of Length Scales: Hybrid Molecular Dynamics and Finite Element Approach for Multiscale Nanodevice Simulations*, Materials Research Society, Boston, pp. 9–3.
[67] Zhigilei, L. V., 2001, *Computational Model for Multiscale Simulation of Laser Ablation*, Materials Research Society, San Francisco, pp. 2–1.
[68] Kim, J. D., and Kim, D. S., 1995, ''Theoretical Analysis of Micro-Cutting

Characteristics in Ultra-Precision Machining,'' J. Mater. Process. Technol., **49**, pp. 387–398.
[69] Vogler, M. P., DeVor, R. E., and Kapoor, S. G., 2004, ''On the Modeling and Analysis of Machining Performance in Micro-Endmilling, Part II: Cutting Force Prediction,'' ASME J. Manuf. Sci. Eng., Proc. ASME Manufacturing Engineering Division (MED-vol. 15), ASME International Mechanical Engineering Congress and Exposition, Anaheim, CA. Paper No. IMECE2004-62416.
[70] Joshi, S., and Melkote, S., 2002, ''An Explanation for the Size-Effect in Machining Using Strain Gradient Plasticity,'' *JSME/ASME Int. Conf. On Materials and Processing*, pp. 318–323.
[71] Liu, X., Jun, M. B. G., DeVor, R. E., and Kapoor, S. G., 2004, ''Cutting Mechanisms and Their Influence on Dynamic Forces, Vibrations and Stability in Micro-Endmilling,'' Proc. ASME Manufacturing Engineering Division (MED-**15**), ASME International Mechanical Engineering Congress and Exposition, Anaheim CA. Paper No. IMECE2004–62416.